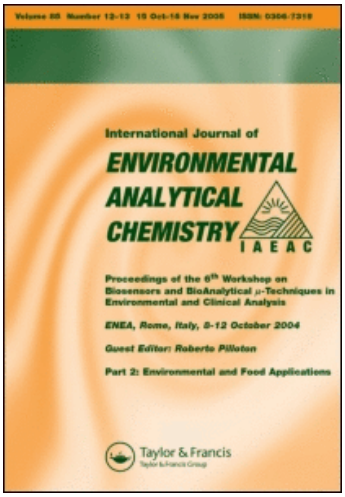

International Journal of Environmental Analytical Chemistry
Publication details, including instructions for authors and subscription information:
http://www.informaworld.com/smpp/title~content=t713640455

Model and real pollutant dispersion: concentration studies by conventional analytics and by laser spectrometry

Zdeněk Zelinger[a]; Michal Střižík[bc]; Pavel Kubát[a]; Kamil Lang[d]; Klára Bezpalcová[b]; Zbyněk Jaňour[b]
[a] J. Heyrovský Institute of Physical Chemistry, Academy of Sciences of the Czech Republic, Dolejškova 3, 182 23 Prague 8, Czech Republic [b] Institute of Thermomechanics, 182 00 Prague 8, Czech Republic [c] Faculty of Safety Engineering, VŠB—Technical University of Ostrava, 700 30 Ostrava-Výškovice, Czech Republic [d] Institute of Inorganic Chemistry, Czech Republic

To cite this Article Zelinger, Zdeněk , Střižík, Michal , Kubát, Pavel , Lang, Kamil , Bezpalcová, Klára and Jaňour, Zbyněk(2006) 'Model and real pollutant dispersion: concentration studies by conventional analytics and by laser spectrometry', International Journal of Environmental Analytical Chemistry, 86: 12, 889 — 903
To link to this Article: DOI: 10.1080/03067310600739590
URL: http://dx.doi.org/10.1080/03067310600739590

Intern. J. Environ. Anal. Chem.
Vol. 86, No. 12, 15 October 2006, 889–903

Model and real pollutant dispersion: concentration studies by conventional analytics and by laser spectrometry

ZDENĚK ZELINGER*†, MICHAL STŘIŽÍK‡§,
PAVEL KUBÁT†, KAMIL LANG¶, KLÁRA BEZPALCOVÁ‡
and ZBYNĚK JAŇOUR‡

†J. Heyrovský Institute of Physical Chemistry, Academy of Sciences of the Czech Republic, Dolejškova 3, 182 23 Prague 8, Czech Republic
‡Institute of Thermomechanics, Academy of Sciences of the Czech Republic, Dolejškova 5, 182 00 Prague 8, Czech Republic
§Faculty of Safety Engineering, VŠB—Technical University of Ostrava, Lumírova 13, 700 30 Ostrava – Výškovice, Czech Republic
¶Institute of Inorganic Chemistry, Academy of Sciences of the Czech Republic, 250 68 Řež, Czech Republic

(*Received 1 July 2005; in final form 20 March 2006*)

The differential absorption LIDAR together with spot analyzers (infrared absorption and chemiluminescence method) was used for concentration measurements in an urban street canyon in Prague. Measurements in the real atmosphere were compared with measurements of concentration distribution inside a model. Experiments in a wind-tunnel-simulated atmosphere were carried out using laser photoacoustic spectrometry and the laser visualization method. A comparison of concentrations on the windward and leeward sides of the model and real street canyon was performed.

Keywords: Air pollution; Photoacoustic spectrometry; Wind tunnel; Differential absorption LIDAR

1. Introduction

Transport vehicles are the major emission source of pollutants in urban areas. This trend is familiar in the countries of the European Community [1–3], and political and related economic changes have also made these developments important in Central and Eastern European countries. The daily traffic level in Prague has increased over the last 10 years by $7–8 \times 10^6$ vehicle-km day^{-1} [4]. This means that car traffic has increased in Prague more than during the entire previous existence of automobile transportation from the end of the 19th century to 1990. Air pollution is becoming a serious problem,

*Corresponding author. Fax: +420-2-8658 23 07. Email: zdenek.zelinger@jh-inst.cas.cz

International Journal of Environmental and Analytical Chemistry
ISSN 0306-7319 print/ISSN 1029-0397 online © 2006 Taylor & Francis
DOI: 10.1080/03067310600739590

and numerous experimental methods have been developed for monitoring atmospheric pollutants [5, 6].

Processes closely connected with air pollution occur mainly in the lower part of the troposphere, designated as the atmospheric boundary layer. This constitutes one of the most complex processes in nature, which can be described by a large number of dependent variables. The most serious problem lies in the fact that movements on various scales occur in the atmosphere. There are movements associated with global circulation, movements of pressure formations, related to changes in the weather, movements in storm formations and air flow in clouds, and movements on the smallest scale [7].

Studies of pollutant transport in the real atmosphere are often expensive and mostly provide only incomplete results. For these reasons, appropriate modelling methods are generally used, which usually consist in mathematical modelling, based on the numerical solution of a set of equations of motion, mass and energy conservation, or methods based on physical modelling in wind tunnels [8–14]. The latter methods use an analogy between processes in the atmospheric boundary layer and processes in the boundary layer formed over the wind tunnel bottom as a basis. Unfortunately, any universal method of simulation does not exist because of different scales, and various methods of approximate simulation must be derived for various types of problems and scales. These modelling methods have advantages and drawbacks, similar to the resolution of many problems in the mechanics of liquids.

Studies in a wind-tunnel-simulated atmosphere provide useful information on the global picture of dispersion of pollutants in urban agglomerates [10–16]. Simulation on a model of future development in the given kind of landscape can prevent structural mistakes from causing the local accumulation of toxic substances in the air of urban agglomerates, and thus directly endangering future inhabitants. Wind-tunnel studies have shown that the entrapment of pollution may be alleviated by distributing high-rise structures along a street, which generates corner vortices mixing pollution upward [16–19]. Qualitative data on processes occurring on the model of street canyons in wind tunnels, often only the concentrations on the side walls of a street canyon, were obtained using various numerical [20, 21] and experimental methods [16–18].

In this paper, we present results of the simulation of an urban street canyon with heavy traffic and a comparison with measurements in the real atmosphere. The street canyon model was built in a wind tunnel, and the model of pollutant emission was created using the line permeation source of methanol vapour. Flow fields were visualized using smoke as a trace and recorded by a video camera light-scattering technique, and pollutant concentration was measured directly by photoacoustic spectrometry. The differential absorption LIDAR method [22] and conventional spot analyzers on the base of infrared absorption and chemiluminescence methods were used for concentration measurements in that part of the real road that corresponded to the model used. We compared differences in concentration in the model and in reality on the windward and leeward sides of the street canyon. The real street canyon is a part of the north–south trunk road that, as a relic of the socialist era, passes through the centre of Prague and remains an unresolved environmental issue for the capital of Czech Republic. The investigation has also been aimed to enrich a basis for studying air pollution along this major motorway.

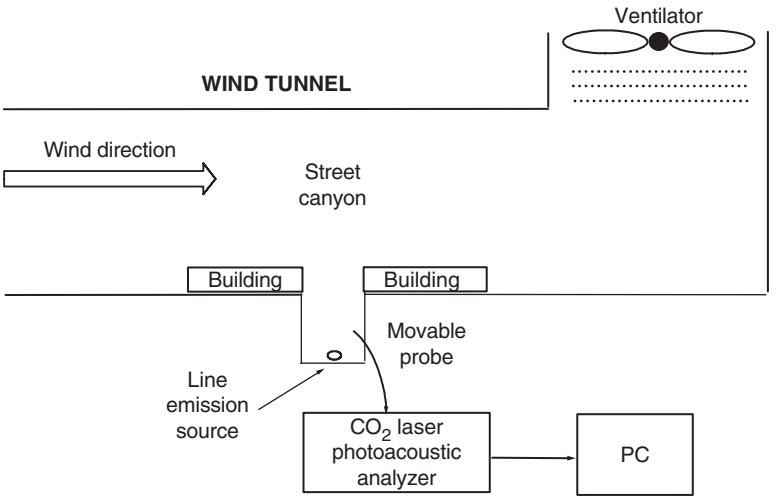

Figure 1. Experimental arrangement of the street canyon model with a line pollutant source in the wind-tunnel concentration measurements by photoacoustic spectrometry.

2. Experimental

2.1 *Model*

The experimental arrangement used for this project is depicted in figure 1. Details of the experimental system have been described in previous papers [23–27]. The model of a symmetric street canyon has an aspect ratio (width of street divided by height of building) of 1.0. Dimensions of working section were $1.5 \times 1.5 \times 2.0$ m. The model was oriented perpendicular to the wind direction. The boundary layer quantities of the incoming boundary layer like roughness length, friction velocity, turbulence intensities, turbulence spectra, etc. on the inlet of the working section corresponded to those of a neutrally stratified rural atmospheric boundary layer. A line pollution source based on the principle of a permeation tube [23] was located in the centre of the model street canyon.

The model was designed with the building height $H = 0.7$ m. Values of Reynolds number $\mathrm{Re} \in (1.5 \times 10^4$ to $6.0 \times 10^5)$ can be attained on the model placed in this wind tunnel. Turbulence elements were situated at the input part of the wind tunnel. A large part of the street canyon model was sunk into the bottom of the wind tunnel (see figure 1). The proposed tasks were the reason for this configuration: a space-resolved cross-field of the concentration inside the street canyon.

Such a configuration could have unfortunate consequences—changes could be expected in dynamic effects of the model on the flow, through the scaling problem and the blocking effect. To investigate the atmosphere inside the street canyon from the point of view of the formation of circulating flows and space resolution, it is necessary to find a compromise configuration to minimize the blocking effect and to maximize the advantages.

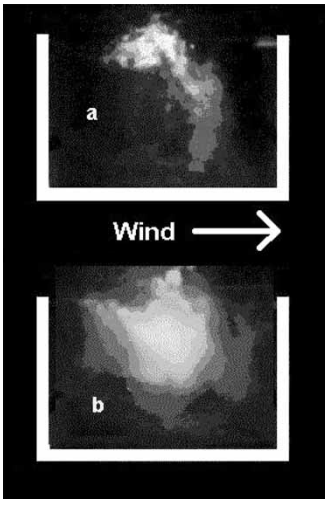

Figure 2. Visualization of the flow inside the street canyon: (a) non-stationary eddy area for lower velocities $U_0 = 2.5\,\mathrm{m\,s^{-1}}$; (b) stationary eddy area shifted in the up-wind direction: $U_0 = 4.5\,\mathrm{m\,s^{-1}}$.

2.2 *Visualization*

The visualization method was employed for the primary qualitative evaluation of flow and to indicate interesting areas for later local measurements. The principle of the visualization system and evaluation of the flow field involves capturing light traces of particles moving in the flow field by using a suitable photosensitive element, the DANTEC light sheet. Particle illumination is provided by the continuous argon laser (1 W power, used in the 'multi-line' mode), whose exit beam is bound in fibres by the optical system. Cylindrical optics form a thin (about 1 mm thick) light wall. The evaluation part of the system consists of an analogue CCIR standard CCD camera with a resolution of 752×582 pixels, optics and frame grabber (PCI cards for the conversion of analogue video signal to digital format, which is further processed by standard graphic software) (figure 2).

A SAFEX smoke generator (DANTEC) was used for particle evolution. It was found that this apparatus was suitable for visualizing a large part of the flow field. An adaptor was developed to visualize a part of the flow field. The smoke was mixed with the compressed air, and this mixture was forced into selected places. This technical apparatus was used for quantitative evaluation of the flow inside the street canyon by Doppler anemometry.

2.3 *Photoacoustic spectrometry*

Sensitive analytical methods are very useful for exact measurements of concentration profiles of pollutants in wind tunnels. For the concentration measurements in the wind tunnel, fast flame-ionization detectors were usually used [28]. In this paper, we present the use of a highly sensitive spectroscopic method with laser photoacoustic detection as an analytical monitoring tool in the wind tunnel. The combination of a CO_2 laser and photoacoustic detection allowed measurements in a linear dynamic range

of up to six orders of magnitude. The $10\,\mu g\,m^{-3}$ detection limit for a model gaseous pollutant (methanol) was achieved in our experimental arrangement. Moreover, the CO_2 laser spectral range did not interfere with the absorption lines of atmospheric H_2O and CO_2; it corresponded to the so-called atmospheric window.

A movable Teflon tube connected through the photoacoustic cell with a pump was used to sample the atmosphere continuously at defined places along the street canyon studied. A continuous flow of samples was taken by the probe; the sampling rate ranged from 3 to $4\,cm^3\,s^{-1}$—these volumes were negligible from the point of view of flow dynamics. The detection unit consisted of the sampling cell—a thermally stabilized brass tube, fitted with an electret microphone, and infrared windows. The infrared radiation of the discretely tunable CO_2 laser (Edinburgh Instruments WL-8-GT) passed through the cell on a pyro-electric detector. The absorption of radiation caused by the presence of absorbing gas led to pressure changes in the cell that were detected by a microphone and then electronically processed. The electronic processing was based on the lock-in amplifiers arranged for the time constant of 1 s; the whole averaging time was 200 s.

2.4 *Differential absorption LIDAR and spot analyzers*

The LIDAR laboratory used in all performed experiments consists of two parts. The first part is the DIAL LIDAR 510M system [29], manufactured by the German company Elight Laser Systems GmbH. The second part is the customary Doppler SODAR PA2 [30], produced in France by REMTECH. The combined DIAL/SODAR system is integrated in a van and equipped with a trailer diesel-powered generator, which makes it fully mobile.

The LIDAR 510M uses a tunable pulse Titan-Sapphire ($Ti^{3+}:Al_2O_3$) laser [31] pumped by xenon flash lamps. The tuning range is 760–880 nm. The pulse duration with a Q-switch is less than 30 ns. A specially designed 'double oscillator' permits alternation (with a repetition rate of 20 Hz) between two wavelengths λ_{on} and λ_{off}, with a bandwidth of less than 0.3 nm each. Non-linear lithium borate (LBO) and barium-β-borate (BBO) crystals are employed in order to generate the second (378–440 nm) and the third (252–293 nm) harmonic frequency. The laser pulse energy, after the third harmonic generation, is more than 0.5 mJ. The backscattered photons collected by a telescope of 400 mm diameter ($f = 1200$ mm) are focused to the monochromator. The signal detected by a high-voltage photo multiplier is digitized by a 12-bit 20 MHz transient recorder. A rotating periscope enables measurement in any direction. Thus, the creation of horizontal or vertical maps of pollutant concentration is possible. In the measurements, the following wavelengths were used: λ_{on} (NO_2) = 398.3 nm and λ_{off} (NO_2) = 397.0 nm. An optogalvanic reference cell (Galvatron) is applied to control the proper tuning of laser emission lines.

The DIAL/SODAR system was located approximately 650 m from the entry of traffic into the street canyon (figure 3). This distance was ideal as regards the geometric compression of the measuring system, influencing the correct evaluation of measured data as one of major factors. The monitored street canyon area was 700 m long. Monitoring was carried out during a working day in the autumn period. In November, the NO_2 vertical distribution was mapped repeatedly by means of two-dimensional vertical scans above the street. The scans through the atmosphere were performed

Figure 3. (a) Legerova Street: a real urban agglomerate street canyon with heavy traffic. (b) Direction of vertical scans above Legerova Street together with locations of DIAL system and spot analyzers schematically shown on the map.

in such manner that they followed the diagonal of the street canyon ground plan. The Doppler SODAR PA2 system (sound detection and ranging) enables continuous measurement of wind speed and direction at heights ranging from 20 to 1500 m. Its measurement is accomplished by emitting a strong acoustic pulse (of central frequency of 2 kHz and acoustic power of 10 W) in four (plus one) different directions and detecting the Doppler frequency shift of the received backscattered echo.

As the local conditions did not allow any direct DIAL determination of down-to-earth pollutant concentration, the continual monitoring of NO_2, NO, and CO was ensured by spot analyzers [32] at the height of 3 m above the pavement surface inside the monitored area. Two spot analyzers located near both canyon walls were used (figure 3).

The monitor APMA-360 was used for carbon monoxide measurements. It is based on cross-flow modulated non-dispersive infrared absorption. The APMA-360 uses solenoid valve modulation. Fixed amounts of the sample gas and the reference gas are injected alternately into the measurement cell. The APMA-360 uses an interference-compensating detector and a flowing reference gas. The reference gas is generated by flowing sample through an oxidation process, where an oxidizing catalyst burns the CO to CO_2. The minimum detection sensitivity of this monitor was 0.05 ppm.

The monitor APNA-360 was used for the continuous monitoring of atmospheric NO_2 and NO concentrations using the cross-flow modulated reduced pressure chemiluminescence method. The APNA-360 uses the combination of the dual cross-flow modulation type chemiluminescence principle and the subtraction calculation method. Standard equipment includes a drier unit with an automatic recycle function to provide dry ambient air as the ozone source. The detector uses a semiconductor sensor

for compactness and long working life. All the necessary features are built into a single rack-sized unit, including a reference-gas generator, an ozone-source drier unit, an ozone decomposer, and a sampling pump. The minimum detection sensitivity of this monitor was 0.05 ppb.

The objective of investigation of NO, NO_2, and CO spatial distribution inside (and above) a real urban agglomerate street canyon was limited to the comparison between concentration levels of the windward and leeward sides. Legerova Street, one of the main through traffic roads of the City of Prague, was chosen as a typical street canyon of urban agglomeration with a well-defined (quasi)line pollution source (figure 3a). There is one-way traffic in the street, and vehicles move slowly in four lines. The width of the canyon, including both sidewalks, is 24 m. The height of linked buildings forming the walls of street canyon is roughly 25 m on the ridge. Thus, the aspect ratio of the street canyon (ratio of street width to height) is approximately 1. However, the canyon of Legerova Street is not fully homogeneous. Its walls are interrupted by crossings with other streets (figure 3b). Typically, during morning rush hours, the frequency of vehicles entering the street canyon can be as high as 60 cars per min.

In the course of monitoring carried out in November, the weather was cloudy, with ground temperatures of around 4°C in the morning. The cloudiness increased during the day, up to an overcast afternoon, with a ground temperature of around 7°C and rain. During the November measuring day, the westerly wind was blowing above the street canyon walls at a speed of 2–6 m s^{-1}, and the speed reached up to 9 m s^{-1} 200 m above the canyon bottom. At the lowest part of the canyon, along its walls, however, only weak southerly ($\pm 5^\circ$) winds were monitored by the anemometer, in the direction of the street axis (1–2 m s^{-1}). The wind direction above the street canyon walls was approximately perpendicular to the street canyon investigated ($\pm 10^\circ$; 20 min averaged values of instantaneous ones measured by SODAR at distances of 25, 100, and 200 m from the bottom). This type of wind direction in the area investigated is not unusual (see the Czech Hydrometeorological Institute website: www.chmi.cz).

3. Results and discussion

The visualization method is demonstrated for a model with $H = 0.7$ m and the aspect ratio of 1 for the quantitative estimation of flow inside the street canyon. A mixture of smoke was emitted into the air stream at the centre of the building edge so that the major part of the mixture could be drawn into the street canyon. The flow field was illuminated by the light wall perpendicular to the axis of the street from a lens located in the roof of the tunnel above the model. The camera was located on the side glass wall to capture the development in the illuminated 2-D flow field in the centre of the street canyon. In this way, a sequence of 'instantaneous' pictures of the flow field inside the street canyon was obtained for Reynolds number values in the interval $\mathrm{Re} \in (2.3 \times 10^4;\ 2.3 \times 10^5)$. The examples of recordings from the video camera are shown in figure 2. From these recordings, the following conclusions can be drawn:

- the flow inside the street, which forms a characteristic eddy, is highly non-stationary (figure 2a), especially for lower velocities;

- with increasing Re, the centre of the eddy area inside the canyon is shifted in the upwind direction (figure 2b).

Our visualizations of pollutant distribution are in accordance with previous results [33]; the importance of the ratio of wall heights was also observed, while the spacing between the walls was less important.

Spatial profiles (figures 4 and 5) of pollutant concentrations from the line source located in the centre of the model street canyon were measured by photoacoustic spectrometry. The values of the concentration measured C ($\mathrm{g\,cm^{-3}}$) were converted to the dimensionless concentration K using the height of the buildings H (cm), the transverse length of the street L (cm), reference wind speed outside the street canyon U ($\mathrm{cm\,s^{-1}}$), and concentration flux of the pollutant line source $Q = (8.3 \times 10^{-5} \pm 2 \times 10^{-6})\,\mathrm{g\,s^{-1}}$ at 20°C, according to the formula:

$$K = \frac{CHUL}{Q}. \tag{1}$$

The coordinates derived from the line-source position are standardized in relation to the overall distance between the source and the buildings, where a negative sign is used to distinguish the leeward side of the street canyon from the windward side of the street.

The pollutant concentrations were measured inside the street canyon for a reference velocity $U = 1.5\,\mathrm{m\,s^{-1}}$ and $\mathrm{Re} = 7 \times 10^4$. The absolute values of standardized concentrations found here vary for the bottom of the street canyon from 4 ($135\,\mu\mathrm{g\,m^{-3}}$) to over 30 ($990\,\mu\mathrm{g\,m^{-3}}$); for the windward wall of the street canyon, the concentration decreases from 6.2 ($230\,\mu\mathrm{g\,m^{-3}}$) to 3.2 ($117\,\mu\mathrm{g\,m^{-3}}$), and for the leeward wall of the street canyon these values diminish from 10 ($380\,\mu\mathrm{g\,m^{-3}}$) to 4 ($150\,\mu\mathrm{g\,m^{-3}}$). The non-dimensional concentration profiles on the leeward and the windward building wall, at the bottom, at a height of 5 cm (2 m above the bottom in reality) and at a height of 20 cm (second floor in reality) of the street canyon with the line emission source in the middle are plotted in figure 4.

The resultant profiles clearly show a substantially higher concentration level on the leeward side of the street, while the opposite windward side of the street is surprisingly efficiently ventilated (figure 4a). It is obvious that the values decrease quite rapidly with increasing height (figure 4b). For illustration, in relation to figure 4, for characteristic Prague buildings from the turn of the 20th century, it can be assumed that the model scale is 1 : 40; the corresponding heights are given in the individual figures for a typical Prague street.

This phenomenon is closely connected with the formation of circulation currents, which shift the pollutants from the windward to the leeward side of the street, where they are accumulated (figure 2). The concentration profiles on the walls of the buildings exhibit a clear decreasing tendency, and the windward side of the street is once again ventilated better than the leeward side. Despite differences in model dimensions, our results of the pollutant dispersion in the two-dimensional street canyon are similar to results observed in [34].

The field of mean non-dimensional concentrations across the street canyon was interpolated from the measured data (figure 5). It can be seen from the figure that the maximum concentration is understandably shifted towards the leeward side at the

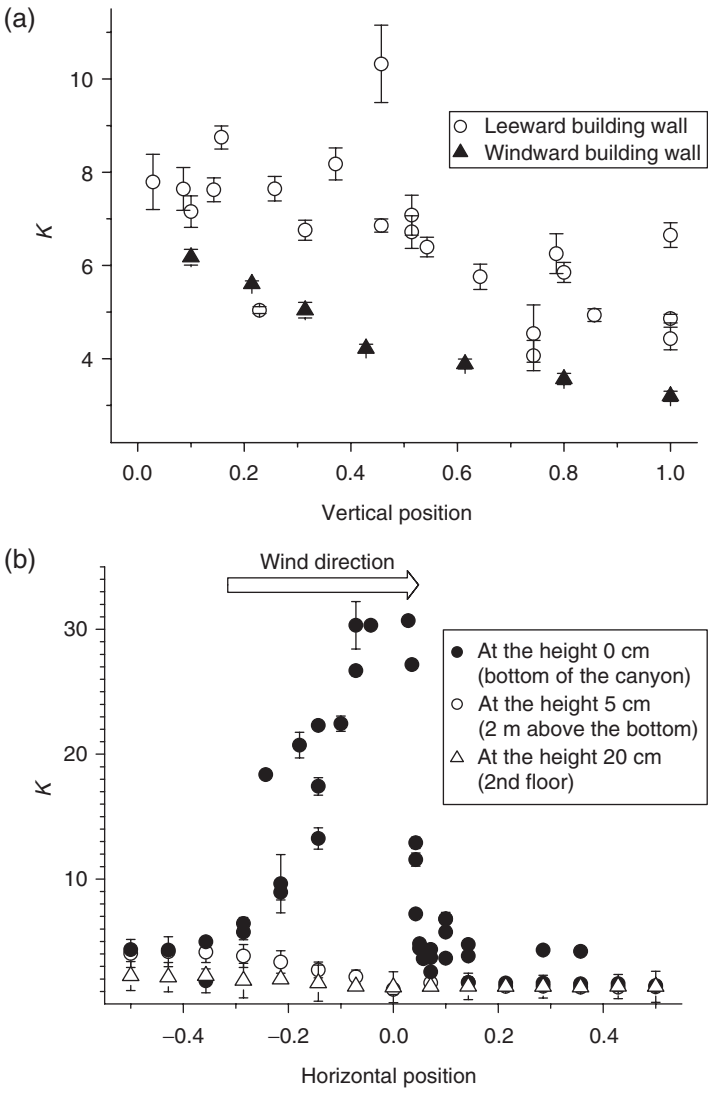

Figure 4. Non-dimensional concentration profile $K = CHU_0\, L/Q$ (equation (1)): (a) on the leeward and the windward building wall and (b) at the bottom, at a height of 5 cm (2 m above the bottom) and 20 cm (2nd floor) in the street canyon with the line emission source in the middle.

bottom of the street. These results of concentration profiles inside the street canyon are in general agreement with findings of other investigators [12].

We paid attention to the verification of validity of the assumption that there is no dependence of flow field on Reynolds number. On selected sites in the vicinity of the line source at the street bottom, concentration measurements were carried out depending upon the reference velocity, and the measured concentration values were converted into dimensionless form according to equation (1). On the basis of these results, it can be assumed that the mean concentration values are independent of the

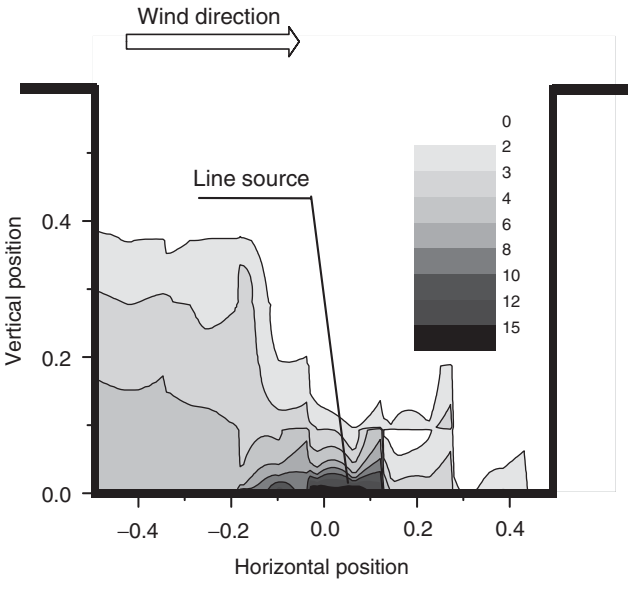

Figure 5. Mean non-dimensional concentration profile $K = CHU_0\ L/Q$ (equation (1)) across the street-canyon.

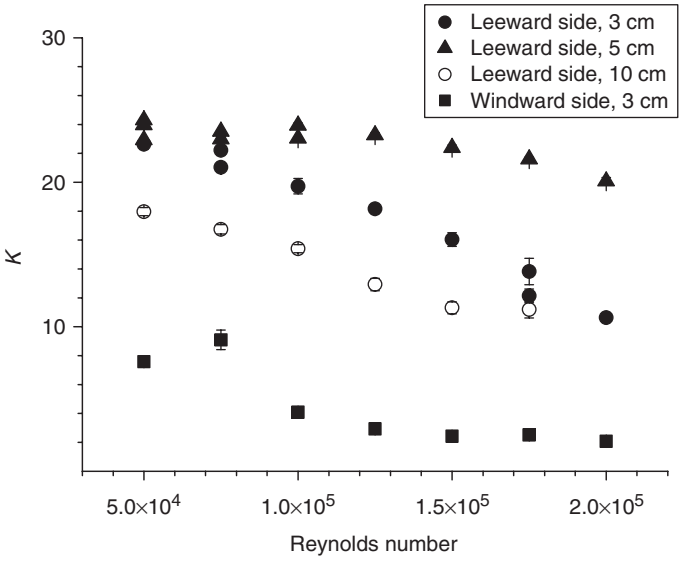

Figure 6. Dependence of non-dimensional concentrations $K = CHU_0\ L/Q$ (equation (1)) around the line emission source (distance from source is indicated in legend) on Reynolds number.

Reynolds number $\mathrm{Re} = H\ U/\nu \geq 1.5 \times 10^4$ except the vicinity of the line source on the leeward side (see figure 6).

The distribution of air pollution could be demonstrated by the ratio of concentration levels on the windward and leeward sides of the street canyon. Our simulation with the

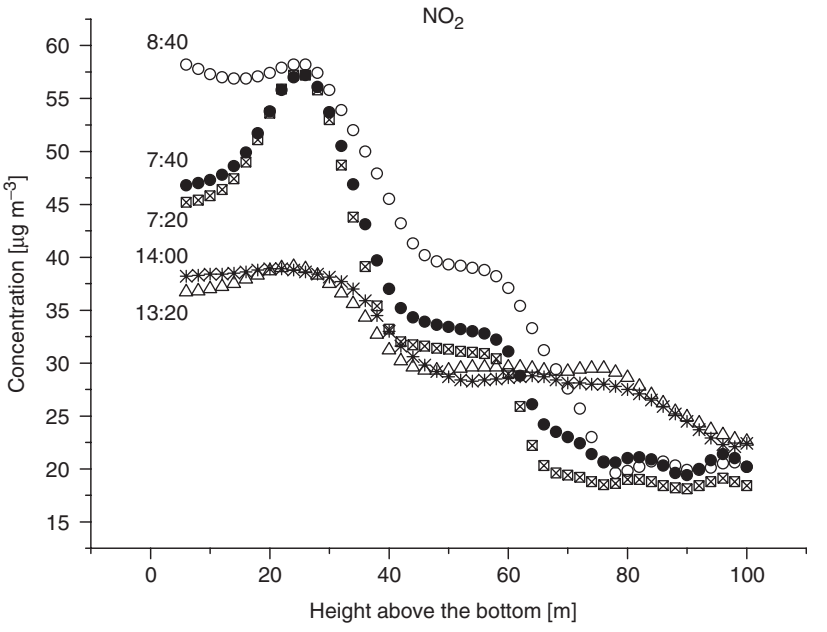

Figure 7. NO_2 concentration dependences on the height above the bottom of the street canyon at different times of the day provided by DIAL.

model of the street canyon predicts (in the case of perpendicular direction of wind flow) higher pollutant concentrations on the leeward side in comparison with the windward side of the canyon (see figures 4 and 5). Figures 4 and 5 show the effect of pollutant accumulation. Near the bottom of the street canyon, the concentration profile is approximately as follows: at the permeation source, the concentrations reach the highest values, and toward the leeward side, the contamination increases by one order of magnitude, filling the bottom of the canyon. The windward side is ventilated better. The effectiveness of ventilation grows with increasing distance from the line source. The figure clearly indicates the great magnitude of contamination to which drivers of slowly moving cars as well as people walking on the leeward side of the street canyon are exposed. These results are very similar to those reported in [11].

We carried out measurements in the real Prague street canyon, and the results of these measurements are shown in figures 7 and 8. During the whole measurement time, a wind above the walls of canyon was perpendicular ($\pm 10^{\circ}$) to the axis of the street, in accordance with modelled conditions. Figure 7 presents time–height–concentration dependences constructed from the 2D vertical scans of NO_2 concentrations provided by DIAL. This means that pollutant concentrations plotted in this figure represent arithmetic means (average time interval ($t - 30$ min; $t + 30$ min)) of instantaneous values detected at corresponding heights of particular scans measured at a corresponding time.

As figure 7 shows, the NO_2 concentration decreases with increasing distance from the street canyon bottom, as predicted by the physical model (figures 4 and 5), and this is in agreement with the results in [12] describing the dispersion of gaseous pollutants in the street canyon. However, a detailed comparison of our results in the simulated and the real atmosphere shows that this concentration decrease is higher in the model than

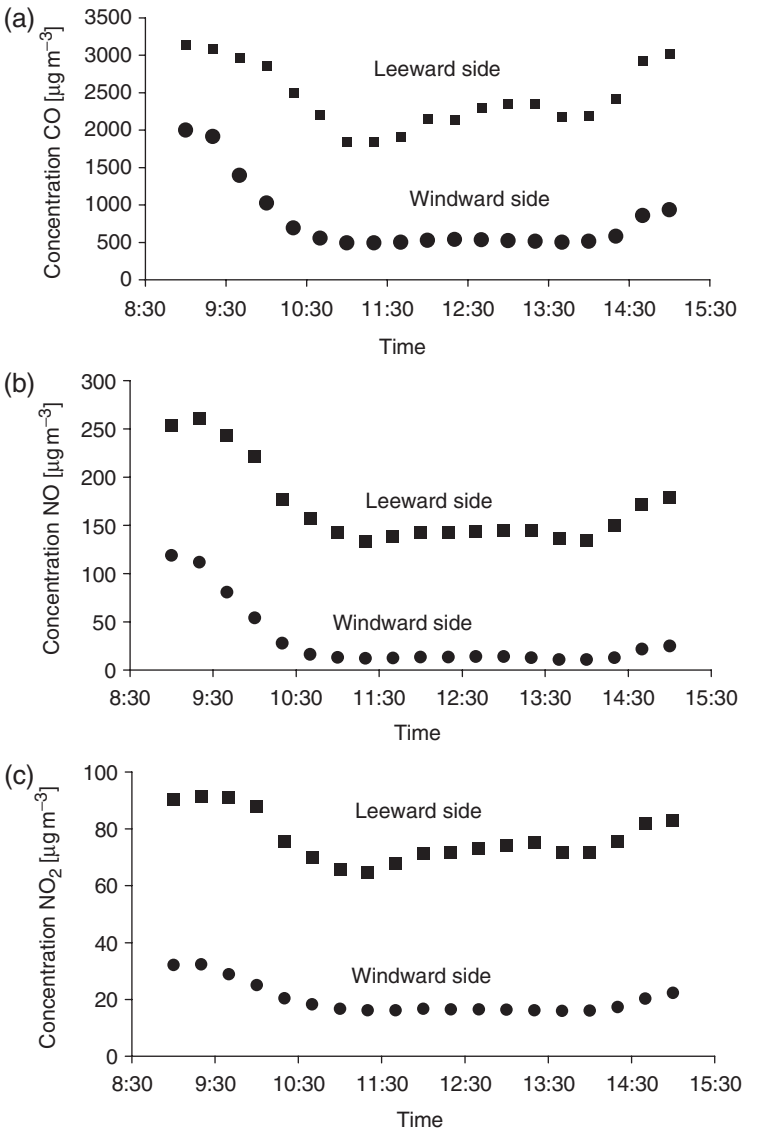

Figure 8. Time distribution of carbon monoxide, nitrogen monoxide, and nitrogen dioxide in figures in the street canyon; Prague: Legerova Street, November.

in reality. One possible cause of discrepancies found could consist in the different geometries of the model and real street canyon (the model of a simple one-lane road *vs.* real quasi-line source consisting of four lines). Using physical modelling, we also investigated a model system of a two-lane motorway whose geometry was closer to the real street canyon investigated and where the resulting spatial distribution of a model pollutant (methanol vapour) was similar to the simple one-lane road model [24]. It is difficult to explain the differences in pollutant distribution observed in the real and model cases based only on the different geometry (a possible thermal effect was

neglected due to the fact that monitoring was performed during the autumn period; physical modelling used the wind tunnel with a thermally non-stratified model of atmospheric boundary layer). This is why we have tried to find a possible interpretation of the difference taking into account chemical processes in the real system. The mixture of nitrogen oxides in automobile exhaust gases consists mainly of nitrogen oxide. The NO is partially oxidized by atmospheric oxygen to NO_2 in hot vehicle exhausts; nevertheless, a competitive reaction of NO with ozone is dominant in the atmosphere under common atmospheric conditions, as it is faster in order of magnitude than for NO oxidation by molecular oxygen. In the morning hours, the ozone concentration reached considerably higher values only at a certain height above the street canyon (80 m above the ground). This might be because of the aforementioned NO reaction with ozone that is consumed during the conversion of NO to NO_2. Thus, with the increasing distance from the ground, the NO_2 concentration does not decrease as predicted by models neglecting possible chemical reactions in the system investigated.

The concentration levels of CO, NO, and NO_2 were monitored by spot analyzers. The results clearly show pollutant concentrations several times higher on the leeward side for all observed pollutants (figure 8). There is some agreement between the simulation (figures 4 and 5) and measurements in the real street canyon. The ratios of pollutant concentration on the leeward and windward side of the street canyon in the case of the model and in reality are approximately of the same order. As the graphs clearly show, the highest concentrations are there at the bottom of the street canyon close to the pollutant source. The increased concentration on the leeward side of the street is also clear. By contrast, the opposite windward side is ventilated more efficiently. This relates to the formation of circulation currents, which move the contamination into the leeward side of the street where it accumulates. The concentration levels decrease with increasing wind speed (figure 6), and the concentrations on the leeward side of the street are higher than those on the windward side (figures 4, 5, and 8). These are the most essential features of pollutant dispersion in the street canyons.

4. Conclusion

The combination of measurements performed in the simulated atmosphere of the wind tunnel and measurements carried out in the real atmosphere has been applied to characterize the circulation of pollutants within the street canyon. The dispersion of the model pollutant (methanol vapour) emitted from a line pollution source was studied in the frame of physical simulations performed in the wind tunnel, where the source was located on the bottom of the urban agglomerate street canyon model. For the first time, the method of CO_2-laser photoacoustic spectrometry has been applied to map the *spatial* distribution of gaseous methanol simulating atmospheric pollution inside a street canyon.

The comparison of pollutant concentrations on the windward and leeward sides was performed for both the model and the real street canyon investigated. At the same time, the pollutant distribution in the vertical profile above the street canyon bottom was studied. In the real system, the NO_2 concentration decreases with increasing distance from the street canyon bottom, as predicted by the physical model of dispersion of

passive gaseous contamination. However, a detailed comparison of our results in the simulated and the real atmosphere shows that this concentration decrease is higher in the model than in reality. The observed effect could be explained on the basis of chemical processes taking place in the real system.

Finally, the effective application of laser analytical techniques (the differential absorption LIDAR based on the Titan-Sapphire laser technique, CO_2-laser photo-acoustic spectrometry) in the sensitive detection of atmospheric pollutants and in the investigation of processes taking place in both the simulated and real atmospheric boundary layer was demonstrated.

Acknowledgements

This work was supported by the Ministry of Education, Youth and Sports of the Czech Republic—projects No. OC723.001, No. OC723.002 (within the framework of the COST 723 action), No. 1P05ME766, and project 1ET400400410 (National Research programme TP2 of the Czech Republic).

References

[1] M. Schatzmann. Air pollution in German cities, paper presented at *Proceedings of the 10th World Clean Air Conference*, Helsinki, Vol. 2, pp. 29–36 (1995).
[2] J.W.W. Longhurst, S.J. Lindley, D.E. Conla, A.F.R Watson. Emissions of air pollutants in the north west region of England, paper presented at *Second International Conference on Air Pollution*, Vol. 2, Barcelona, pp. 106–112 (1994).
[3] C.W.A. Evers. Analysis of emission data with respect to environmental policy in The Netherlands, paper presented at *Second International Conference on Air Pollution*, Vol. 2, Barcelona, pp. 99–106 (1994).
[4] The Yearbook of Transportation Prague 2002. Institute of Transportation Engineering of the City of Prague, Prague (2003). Available online at: http://www.udi-praha.cz/rocenky/Yearbk02/aro2002.htm (accessed 2003).
[5] R.A. Meyers (Ed.). *Encyclopedia of Environmental Analysis and Remediation*, Wiley, New York (1998).
[6] M. Navazo, N. Durana, L. Alonso, J.A. Garcia, J.L. Ilardia, M.C. Gomez, G. Gangoiti. *Int. J. Environ. Anal. Chem.*, **83**, 199 (2003).
[7] A.A. Kolmogorov, *C. R. Acad. Sci U.R.S.S.*, **31**, 538 (1941).
[8] R. Berkowitz. In *Urban Air Pollution—European Aspects*, J. Fenger, O. Hertel, F. Palmgren (Eds), Kluwer Academic, London (1998).
[9] J.E. Cermak. *AIAA J.*, **9**, 1746 (1971).
[10] A.K. Namdeo, J.J. Colls, C.J. Baker. *Sci. Total Environ.*, **235**, 3 (1999).
[11] W. Pearce, C.J. Baker. *J. Wind Eng. Ind. Aerodyn.*, **80**, 327 (1999).
[12] G. Dezsö-Weidinger, A. Stitou, J. van Beeck, M.L. Riethmuller. *J. Wind Eng. Ind. Aerodyn.*, **91**, 1117 (2003).
[13] P. Kastner-Klein, E. Fedorovich, M.W. Rotach. *J. Wind Eng. Ind. Aerodyn.*, **89**, 849 (2001).
[14] P. Kastner-Klein, E.J. Plate. *Atmos. Environ.*, **33**, 3973 (1999).
[15] J.E. Cermak. *Wind Climata in Cities*, p. 383, Kluwer Academic, London (1995).
[16] B.M. Leitl, R.N. Meroney. *J. Wind Eng. Ind. Aerodyn.*, **67–68**, 293 (1997).
[17] J.B. Wedding, D.J. Lambert, J.E. Cermak. *Air Pollut. Control Assoc. J.*, **27**, 557 (1977).
[18] S. Rafailids, M. Schatzmann. In *Proceedings of the 21st International Meeting on Air Pollution Modelling and Its Applications*, pp. 56–68, Baltimore, MD (1995).
[19] W.G. Hoydysh, R.A. Griffiths, Y. Ogawa. A scale model study of the dispersion of pollution in street canyons, paper presented at *67th Annual Meeting of the Air Pollution Control Association*, Denver, CO, paper no. 74–157 (1974).
[20] R. Hwang, Y.C. Chow, Y.F. Peng. *Int. J. Numer. Meth. Fluids*, **31**, 767 (1999).
[21] Y.Q. Zhang, A.H. Hubert, S.P.S. Arya, W.H. Snyder. *J. Wind Eng. Ind. Aerodyn.*, **46–47**, 129 (1993).

[22] S. Svanberg. In *Air Monitoring by Spectroscopic Techniques*, M.W. Sigrist (Ed.), pp. 85–161, Wiley, New York (1994).
[23] Z. Zelinger, S. Civiš, Z. Jaňour. *Analyst*, **124**, 1205 (1999).
[24] S. Civiš, Z. Zelinger, M. Střižík, Z. Jaňour. *NATO Science Series II: Mathematics, Physics and Chemistry*, Vol. 20, pp. 275–299, Kluwer Academic, Dordrecht (2001).
[25] S. Civiš, M. Střižík, Z. Jaňour, J. Holpuch, Z. Zelinger. *J. AOAC Int*., **85**, 1 (2002).
[26] Z. Zelinger, M. Střižík, P. Kubát, Z. Jaňour, P. Berger, A. Černý, P. Engst. *Opt. Las. Eng*., **42**, 403 (2004).
[27] Z. Jaňour, J. Holpuch, M. Střižík. In *EUROMECH Col. 391, Wind Tunnel Modelling of Dispersion in Environmental Flows*, Z. Jaňour, J. Holpuch (Eds), pp. 17–18, Institute of Thermomechanics AS CR, Prague (1999).
[28] M. Pavageau, M. Schatzmann. *Atmos. Environ*., **33**, 3961 (1999).
[29] Elight Laser Systems GmbH. Teltow. *LIDAR 510M Handbuch*, 2000. Available online at: www.elight.de (accessed 2003).
[30] Remtech Inc. Fort Collins. *The Operation and Maintenance Manual for the PA1, PA2, PA1-LR, and RASS, 2000*. Available online at: www.remtechinc.com (accessed 2002).
[31] J. Kolenda. *Anwendungen des blitzlampengepumpten Titan: Saphir Lasers in der LIDAR-Technik: Doktorarbeit*, Freie Universität, Berlin (1993).
[32] Horiba Europe GmbH Tulnn. 1992. Available online at: http://www.horiba.de/ (accessed 2003).
[33] F. Gerdes, D. Olivari. *J. Wind Eng. Ind. Aerodyn*., **82**, 105 (1999).
[34] A.P.G. Sagrado, J. van Beeck, P. Rambaud, D. Olivari. *J. Wind Eng. Ind. Aerodyn*., **90**, 321 (2002).